Magnetic Helicities in Solar Active Regions

Stéphane RÉGNIER

based on

”Self and Mutual Helicities in Coronal Magnetic Configurations”

S. Régnier, T. Amari, R. C. Canfield 2005, A&A, 442, 345

- Definitions

- Helical structures in the Sun atmosphere

  - $\star$ from the convection zone
  - $\star$ on the photosphere
  - $\star$ in the corona
  - $\star$ in the interplanetary medium

- Self and Mutual helicities in active regions

Definitions

Helicity of $\vec{\phi}$:

$$H = \int_\Omega \vec{\phi} \cdot \vec{\nabla} \wedge \vec{\phi} \, d\Omega$$

Definitions

Helicity of $\vec{\phi}$:

$$H = \int_{\Omega} \vec{\phi} \cdot \vec{\nabla} \wedge \vec{\phi} \; d\Omega$$

Magnetic Helicity:

$$H_m = \int_{\Omega} \vec{A} \cdot \vec{B} \; d\Omega = \int_{\Omega} \vec{A} \cdot \vec{\nabla} \wedge \vec{A} \; d\Omega$$

Definitions

Helicity of $\vec{\phi}$:

$$H = \int_\Omega \vec{\phi} \cdot \vec{\nabla} \wedge \vec{\phi} \; d\Omega$$

Magnetic Helicity:

$$H_m = \int_\Omega \vec{A} \cdot \vec{B} \; d\Omega = \int_\Omega \vec{A} \cdot \vec{\nabla} \wedge \vec{A} \; d\Omega$$

Current Helicity:

$$H_c = \int_\Omega \mu_0 \, \vec{j} \cdot \vec{B} \; d\Omega = \int_\Omega \vec{B} \cdot \vec{\nabla} \wedge \vec{B} \; d\Omega$$

Definitions

Helicity of $\vec{\phi}$:

$$H = \int_{\Omega} \vec{\phi} \cdot \vec{\nabla} \wedge \vec{\phi} \; d\Omega$$

Magnetic Helicity:

$$H_m = \int_{\Omega} \vec{A} \cdot \vec{B} \; d\Omega = \int_{\Omega} \vec{A} \cdot \vec{\nabla} \wedge \vec{A} \; d\Omega$$

Current Helicity:

$$H_c = \int_{\Omega} \mu_0 \; \vec{j} \cdot \vec{B} \; d\Omega = \int_{\Omega} \vec{B} \cdot \vec{\nabla} \wedge \vec{B} \; d\Omega$$

Kinetic Helicity:

$$H_k = \int_{\Omega} \vec{v} \cdot \vec{w} \; d\Omega = \int_{\Omega} \vec{v} \cdot \vec{\nabla} \wedge \vec{v} \; d\Omega$$

Relative magnetic helicity

$\vec{A}$ is not gauge invariant:

$$\vec{A}' = \vec{A} + \vec{\nabla}\phi \quad \rightarrow \quad H_m(\vec{B}, \vec{A}) \neq H_m(\vec{B}, \vec{A}')$$

Relative magnetic helicity:

$$\Delta H_m = \int_\Omega \, (\vec{A} - \vec{A}_0) \cdot (\vec{B} + \vec{B}_0) \; d\Omega - \int_\Sigma \, \chi \, (\vec{B} + \vec{B}_0) \cdot \vec{n} \; d\Sigma$$

(Berger and Field 1984, J. Fluid Mech. 147, 133)

$$\Delta H_m = \int_\Omega \, (\vec{A} + \vec{A}_0) \cdot (\vec{B} - \vec{B}_0) \; d\Omega$$

(Finn and Antonsen 1985, Plasma Phys. Controlled Fusion, vol.9, 3, 111)

Force-free Fields and Magnetic Helicity

For a linear force-free field,

$$\vec{\nabla} \wedge \vec{B} = \alpha \vec{B}$$

where α is a constant in the volume Ω given by

$$\alpha = \frac{1}{B_z} \left(\frac{\partial By}{\partial x} - \frac{\partial B_x}{\partial y} \right)$$

We have

$$H_c = 2\mu_0 \alpha E_m$$

and

$$2\mu_0 \frac{d(E_m(lff) - E_m(pot))}{d(\Delta H_m)} = \alpha$$

(from Kusano et al. 2002, ApJ, 577, 501)

Basically, α has the same sign as the magnetic helicity

Self and Mutual Helicities (1)

Magnetic helicity in an open volume:

Following Berger (1999), the magnetic field can be decomposed into two fields inside a volume Ω with a surface boundary Σ,

$$\vec{B} = \vec{B}_{cl} + \vec{B}_{ref}$$

where $\vec{\nabla} \wedge \vec{B}_{ref} = \vec{0}$ and $\vec{B} \cdot \vec{n} = \vec{B}_{ref} \cdot \vec{n}$ on the surface Σ.

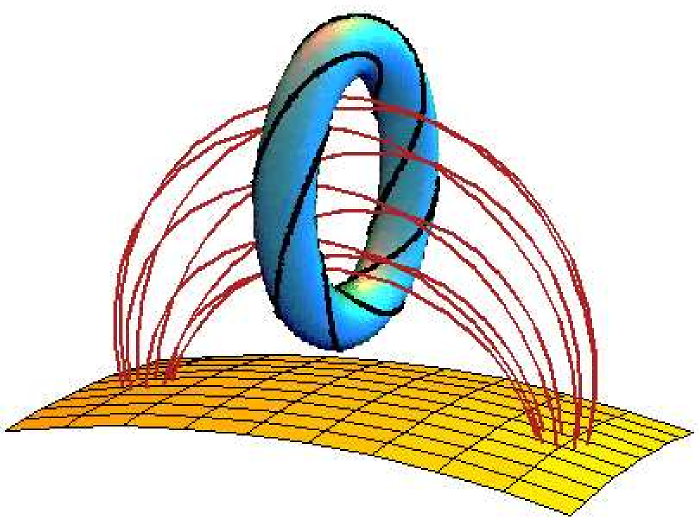

$\vec{B}_{cl}$: closed field pictured as the blue torus;
$\vec{B}_{ref}$: a reference field or potential field.

Self and Mutual Helicities (2)

The magnetic helicity can be re-written as follows:

$$H_m(\vec{B},\vec{A}) = H_m(\vec{B}_{cl},\vec{A}_{cl}) + 2H_m(\vec{B}_{cl},\vec{A}_{ref}) + H_m(\vec{B}_{ref},\vec{A}_{ref})$$

where we define the *self helicity* as

$$H_{self} = H_m(\vec{B}_{cl},\vec{A}_{cl}) = \int_\Omega \vec{A}_{cl}\cdot\vec{B}_{cl}\ d\Omega$$

and the *mutual helicity* as

$$H_{mut} = 2H_m(\vec{B}_{cl},\vec{A}_{ref}) = 2\ \int_\Omega \vec{A}_{ref}\cdot\vec{B}_{cl}\ d\Omega$$

We also define the *vacuum helicity* (or self helicity of the reference field) as

$$H_{vac} = H_m(\vec{B}_{ref},\vec{B}_{ref}) = \int_\Omega \vec{A}_{ref}\cdot\vec{B}_{ref}\ d\Omega$$

Helicity Transport (1)

Following Heyvaerts and Priest (1984), one can derive the rate of change of the magnetic helicity in a volume V including dissipative terms:

$$\begin{aligned}\frac{dH}{dt} &= \oint_{\Sigma} (\vec{B}\cdot\vec{A})\vec{v}\cdot\vec{n}\ d\Sigma + \oint_{\Sigma} (\vec{v}\cdot\vec{A})\vec{B}\cdot\vec{n}\ d\Sigma \\ &\quad -2\int_{V}\frac{1}{\sigma}\ \vec{B}\cdot\vec{J}\ dV + \int_{\Sigma}\frac{1}{\sigma}\ \vec{A}\wedge\vec{J}\ d\Sigma\end{aligned}$$

In ideal MHD, Berger and Field (1984) have shown the rate of change of helicity can be re-written as follows:

$$\frac{d}{dt}\Delta H_m = 2\ \int_{\Sigma}\ (\vec{v}_t\cdot\vec{A}_{ref})\ \vec{B}\cdot\vec{n}\ d\Sigma - 2\ \int_{\Sigma}\ (\vec{B}_t\cdot\vec{A}_{ref})\ \vec{v}\cdot\vec{n}\ d\Sigma$$

where $\vec{A}_{ref}$ is the unique vector potential satisfying

$$\vec{\nabla}\wedge\vec{A}_{ref}\cdot\vec{n} = B_n, \qquad \vec{\nabla}\cdot\vec{A}_{ref} = 0, \qquad \vec{A}_{ref}\cdot\vec{n} = 0$$

($\vec{n}$ is the normal vector to the surface pointing outside the volume)

Helicity Transport (2)

Therefore, the first term measures the transport of magnetic helicity through the surface, and the second term measures the effect of boundary motions (transverse motions to the surface).

By replacing $\vec{v}$ by $\vec{u}$, Berger and Démoulin (2002) have shown that

$$\frac{d}{dt}\Delta H_m = 2\int_{\Sigma} (\vec{u}\cdot\vec{A}_{ref})\vec{B}\cdot\vec{n}\ d\Sigma$$

$vecu$ being the photospheric footpoint motions measured basically by local correlation tracking, $\vec{v}$ being the plasma velocity:

$$\vec{u} = \vec{v}_t - \frac{v_n}{B_n}\vec{B}_t$$

- Definitions

- Helical structures in the Sun atmosphere

  ⋆ from the convection zone

  ⋆ on the photosphere

  ⋆ in the corona

  ⋆ in the interplanetary medium

- Self and Mutual helicities in active regions

Emergence of flux rope from the convection zone through the photosphere

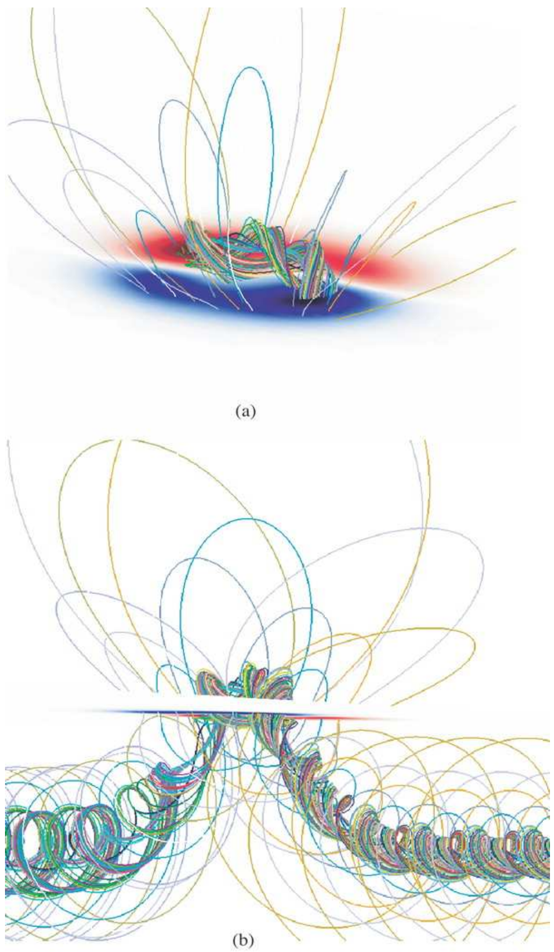

Emergence of a twisted flux tube generated in the convection zone through the photospheric surface (from Amari et al. 2005).

Evidence of helical structures at the photospheric level by measuring the transverse magnetic field components or the value of α (force-free parameter) at a given location (e.g. Krall et al. 1982, Solar Phys., 79, 59), or by looking at the long-term evolution of active regions (López Fuentes et al. 2000, ApJ, 544, 540)

On the photosphere: measure of α

The force-free parameter α can be derived from vector field measurements or by comparing with a linear force-free field extrapolation:

From vector fields: the α parameter is derived locally (at each pixel) from

$$\alpha = \frac{1}{B_z} \left(\frac{\partial B_y}{\partial x} - \frac{\partial B_x}{\partial y} \right)$$

Averaged or mean values of α are used as proxies for the magnetic helicity (e.g., Leka 1999) as well as to established the hemispheric rule (left-handed in the northern hemisphere, right-handed in the southern hemisphere, Canfield and Pevtsov 2000)

From lfff: Démoulin et al (2002) and Green et al. (2002) have derived the α from a linear force-free field comparing with soft X-ray data, and then estimated the magnetic helicity following the expression given by Berger (1985).

On the photosphere: rate of change

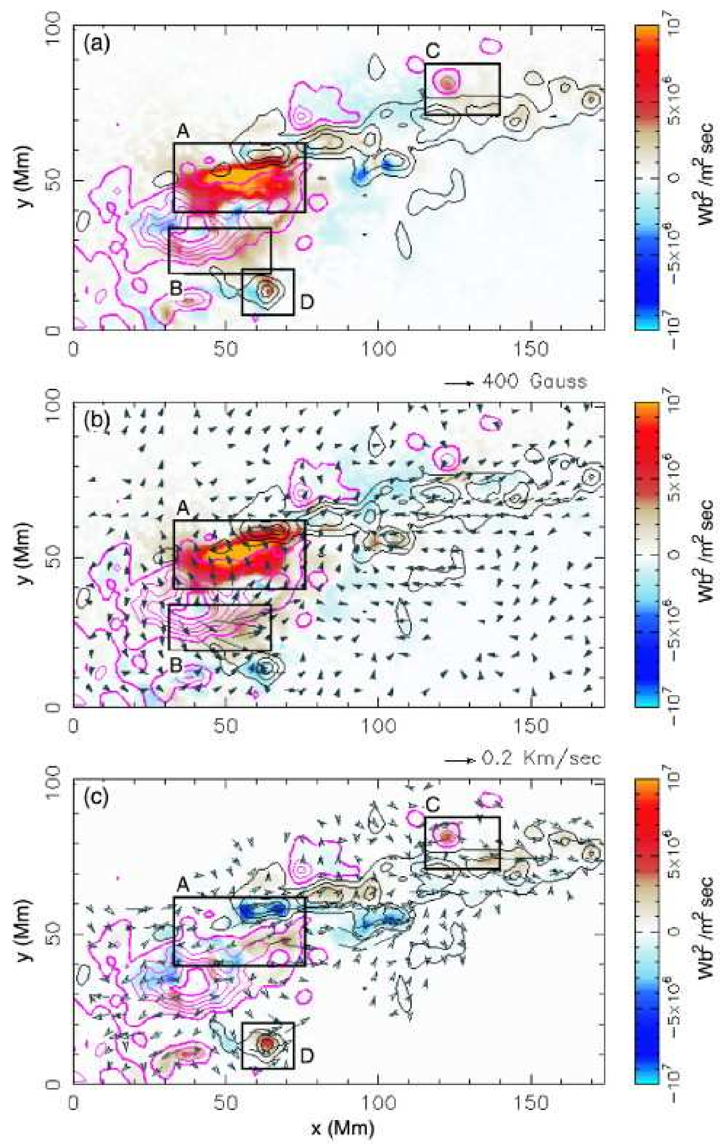

The magnetic helicity rate of change associated with transverse motions can be derived from line-of-sight magnetograms, using a local correlation tracking technique to compute the transverse velocity field. Kusano et al. (2002) have developed a technique by combining line-of-sight measurements to derive the transverse velocity, vector magnetograms for the 3 components of $\vec{B}$ and the induction equation for the vertical component of the velocity. See Figure on the left for the total helicity rate (top), due to vertical motions (middle), due to horizontal motions (bottom)

Flux rope observed in the corona (1)

Filaments/prominences as well as sigmoids are considered as twisted flux tubes. The measurement of the shear angle can give an estimate of the α parameter in a thin flux tube approximation.

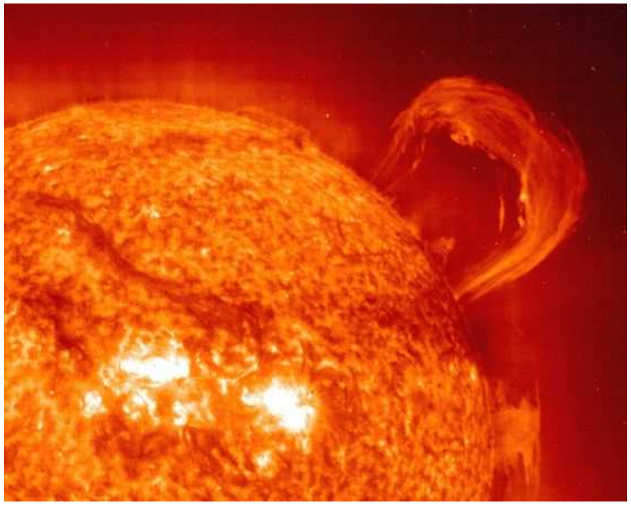

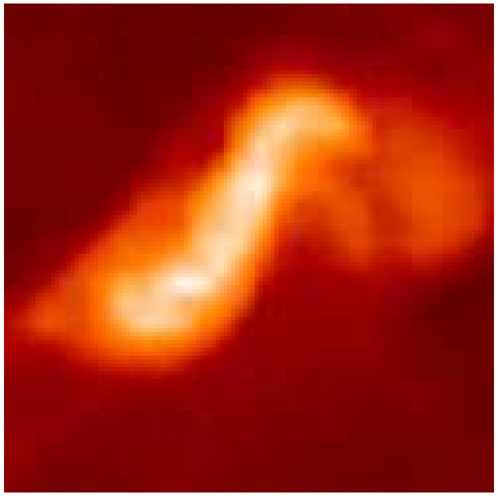

Flux rope observed in the corona (2)

Using nonlinear force-free field reconstruction, we (Régnier et al. 2002, 2004) have evidenced twisted flux tubes in magnetic configurations with different twist and different handedness.

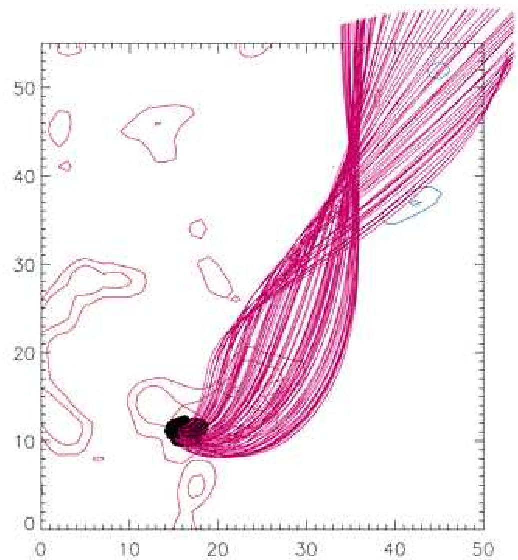

	Filament	Sigmoid	Quasi-potential	Highly twisted
α (Mm^{-1})	0.15	-0.15	-6 10^{-3}	0.03
J_z ($mA.m^{-2}$)	2.4	-2.3	-0.7	3.5
L (Mm)	205	180	220	169
h (Mm)	34	45	54	61
θ_s	5^o	5^o	50^o	75^o
B_h (G)	49	56	20	36
N	0.5–0.6		0	1.1–1.2
Magnetic Dips	Yes	No	No	No

Flux rope in the interplanetary medium as a consequence of CME

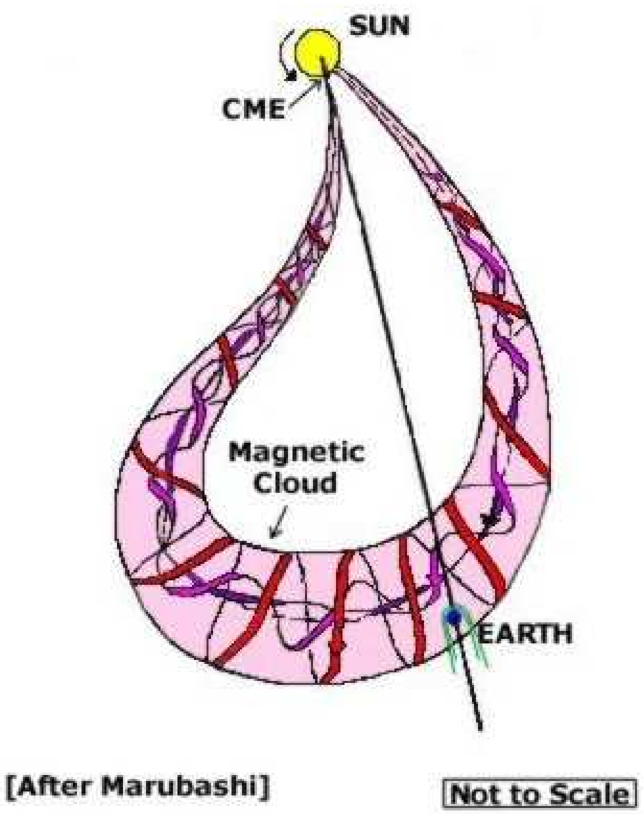

Ejection of a twisted flux tube or magnetic cloud from the low corona into the interplanetary medium.
Evidence of helical structures by in-situ measurements of the magnetic field components. The α value is derived from a model of flux rope in cylindrical coordinates (e.g., Lundquist solutions–linear force-free field, Gold-Hoyle solutions–nonlinear force-free field with uniform twist

- Definitions

- Helical structures in the Sun atmosphere
  - $\star$ from the convection zone
  - $\star$ on the photosphere
  - $\star$ in the corona
  - $\star$ in the interplanetary medium

- Self and Mutual helicities in active regions

Aim and Method

- Determining the magnetic helicity including self and mutual helicities from nonlinear force-free field (nlfff) extrapolation technique

- nlff numerical scheme based on Grad-Rubin method re-written in terms of the vector potential

- study of two simple cases (one with a twisted flux tube, one with a simple topology) and a solar active region

Extended Gold & Hoyle solutions (1)

The Gold & Hoyle (1960) solutions describe a set of nonlinear force-free fields representing a uniformly twisted flux tube.

$$B_z(r) = \frac{B_0}{1+q^2r^2}, \qquad B_\theta(r) = \frac{B_0 q r}{1+q^2r^2}, \qquad \alpha(r) = \frac{2q}{1+q^2r^2},$$

where q characterizes the twist (unit of $1/r$).

We define an extended set of nonlinear force-free fields describing a non-uniformly twisted flux tube:

$$B_z = \frac{B_0}{\left(1+\kappa\frac{r^2}{r_0^2}\right)^{\kappa}}, \qquad B_\theta = \pm\frac{B_0}{\sqrt{\kappa(2\kappa-1)}}\,\frac{r_0}{r}\,\left[1-\frac{1+2\kappa^2\frac{r^2}{r_0^2}}{\left(1+\kappa\frac{r^2}{r_0^2}\right)^{2\kappa}}\right]^{\frac{1}{2}}$$

where κ and r_0 are two free parameters. Solutions exist only for $\kappa > \frac{1}{2}$

Extended Gold & Hoyle solutions (2)

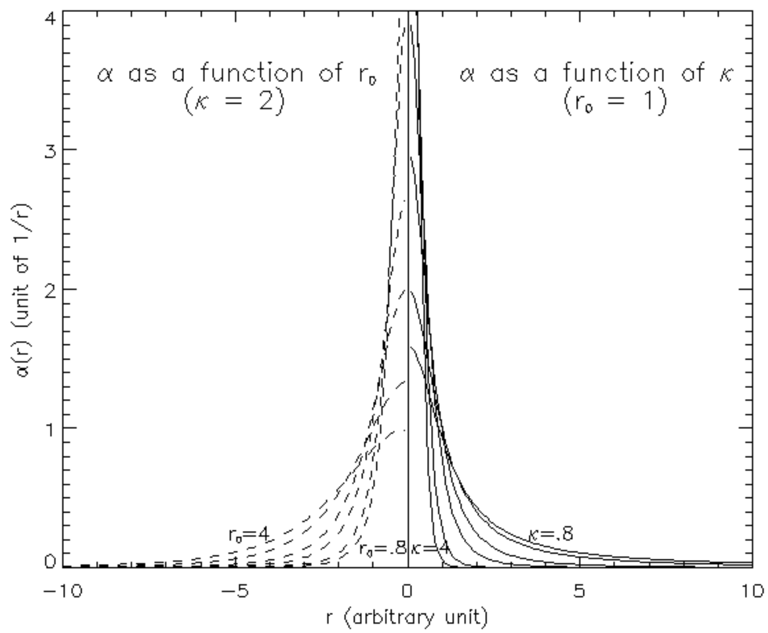

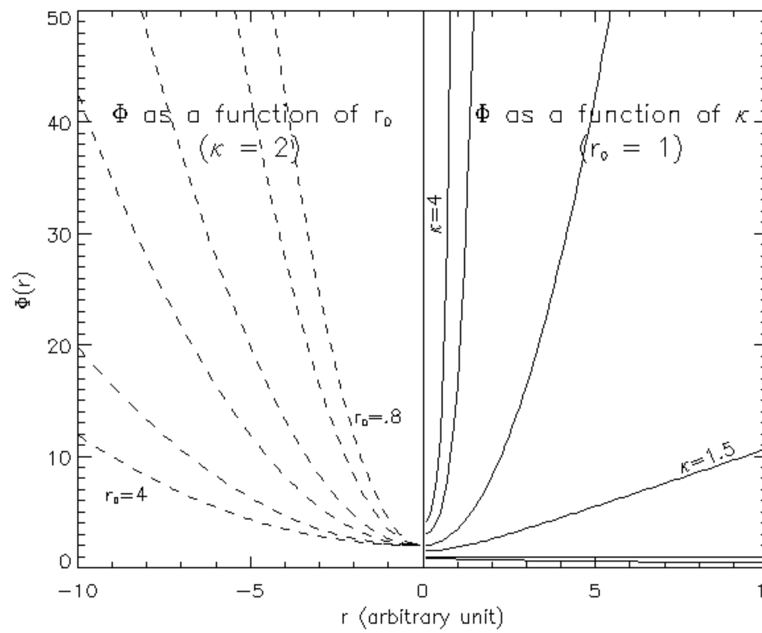

Left: α as a function of the characteristic thickness r_0 (dashed curves) for $r_0 = 0.8, 1, 1.5, 2, 3, 4$ and as a function of κ (solid curves) for $\kappa = 0.8, 1, 1.5, 2, 3, 4$

Right: Same as for the left plot for $\Phi = \frac{r_0 B_\theta}{r B_r}$, the twist function

Extended Gold & Hoyle solutions (3)

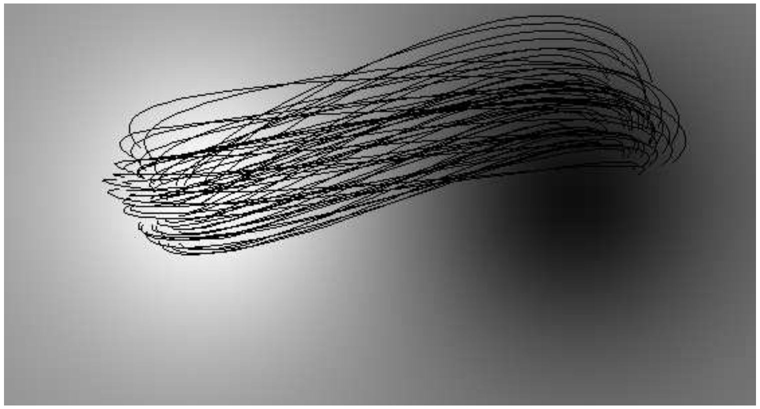

Typical nonlinear force-free field distribution reconstructed from the extended Gold & Hoyle solution.

EG&H solutions	$H_{self}(\vec{B}_{cl})$	$H_{mut}(\vec{B}_{pot}, \vec{B}_{cl})$	ΔH_m	$H_{self}(\vec{B}_{pot})$
$\kappa = 0.8$, $r_0 = 0.56$	0.13 (2.2%)	5.6 (96%)	5.8	-3.7 10^{-4} (6 10^{-3}%)
$\kappa = 0.8$, $r_0 = 0.4$	0.38 (4.4%)	8.2 (96%)	8.5	-3.7 10^{-4} (4 10^{-3}%)
$\kappa = 2$, $r_0 = 1.4$	0.15 (2.9%)	4.8 (95%)	5.1	-3.4 10^{-4} (7 10^{-3}%)
$\kappa = 2$, $r_0 = 1$	0.44 (5.8%)	7.2 (94%)	7.6	-3.4 10^{-4} (4 10^{-3}%)

Magnetic helicities for 4 different EG&H solutions (unit of 10^{43} $G^2.cm^4$). The percentage in parenthesis is computed with respect to the relative helicity.

Three-source configuration

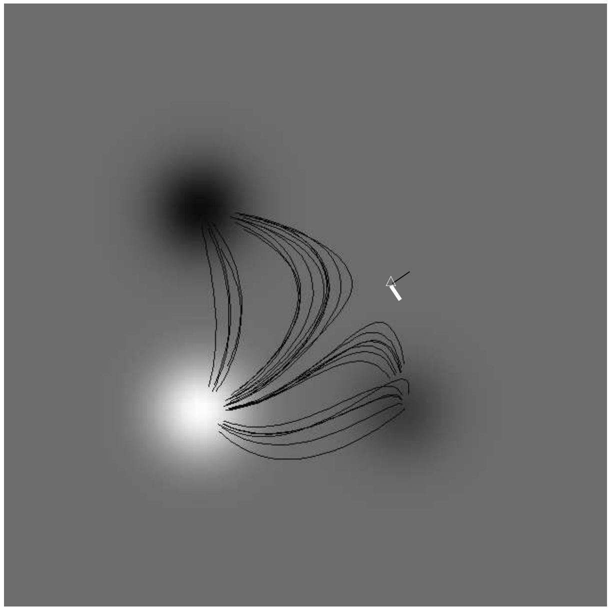

Distribution of magnetic field with three balanced sources (see e.g. Brown & Priest 1999). The configuration has a topology: one negative null (triangle), spine and fan directions are indicated by the white and the black lines respectively

Trisources	$H_{self}(\vec{B}_{cl})$	$H_{mut}(\vec{B}_{pot}, \vec{B}_{cl})$	ΔH_m	$H_{self}(\vec{B}_{pot})$
$\alpha = 0.04$	$7.92\ 10^{-5}$ (34%)	$9.08\ 10^{-5}$ (62%)	$1.45\ 10^{-4}$	$4.9\ 10^{-5}$ (33%)
$\alpha = 0.08$	$1.24\ 10^{-3}$ (86%)	$2.44\ 10^{-4}$ (16%)	$1.44\ 10^{-3}$	$4.9\ 10^{-5}$ (3.5%)

Magnetic helicities for 2 linear force-free configurations (unit of 10^{43} $G^2.cm^4$). α unit is Mm^{-1}. The percentage in parenthesis is computed with respect to ΔH_m.

Active region 8210 (1)

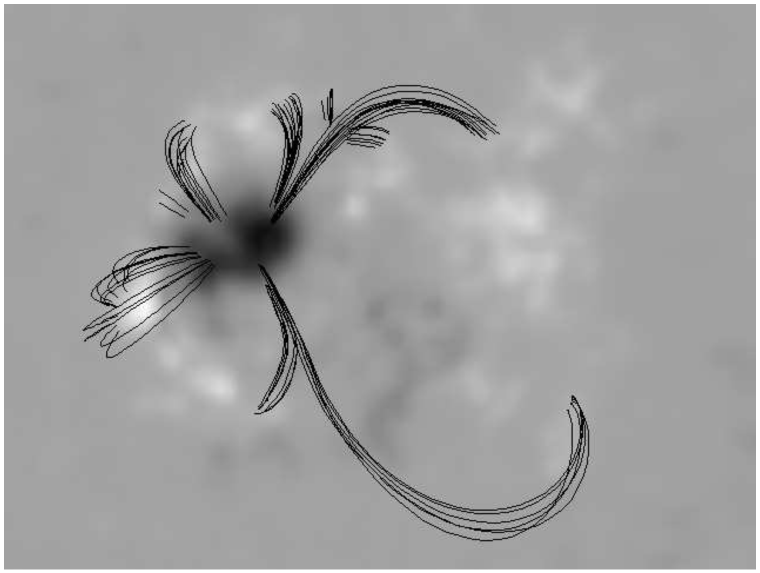

Nonlinear force-free configuration of AR 8210 using photospheric boundary conditions provided by one MSO/IVM vector magnetogram observed at 19:40 UT on May 1st 1998.

AR 8210	$H_{self}(\vec{B}_{cl})$	$H_{mut}(\vec{B}_{pot}, \vec{B}_{cl})$	ΔH_m	$H_{self}(\vec{B}_{pot})$
at 19:40 UT	-8.8 10^{-2} (21%)	-0.36 (86%)	-0.42	2 10^{-2} (4.7%)

Magnetic helicities for AR8210 at 19:40 UT on May 1st 1998 (unit of 10^{43} $G^2.cm^4$). The percentage in parenthesis is computed with respect to ΔH_m.

Active region 8210 (2)

We follow the evolution of the magnetic helicities during ∼4 hours with one vector magnetogram every 15 min (see Régnier and Canfield 2006, A&A, 451, 319).

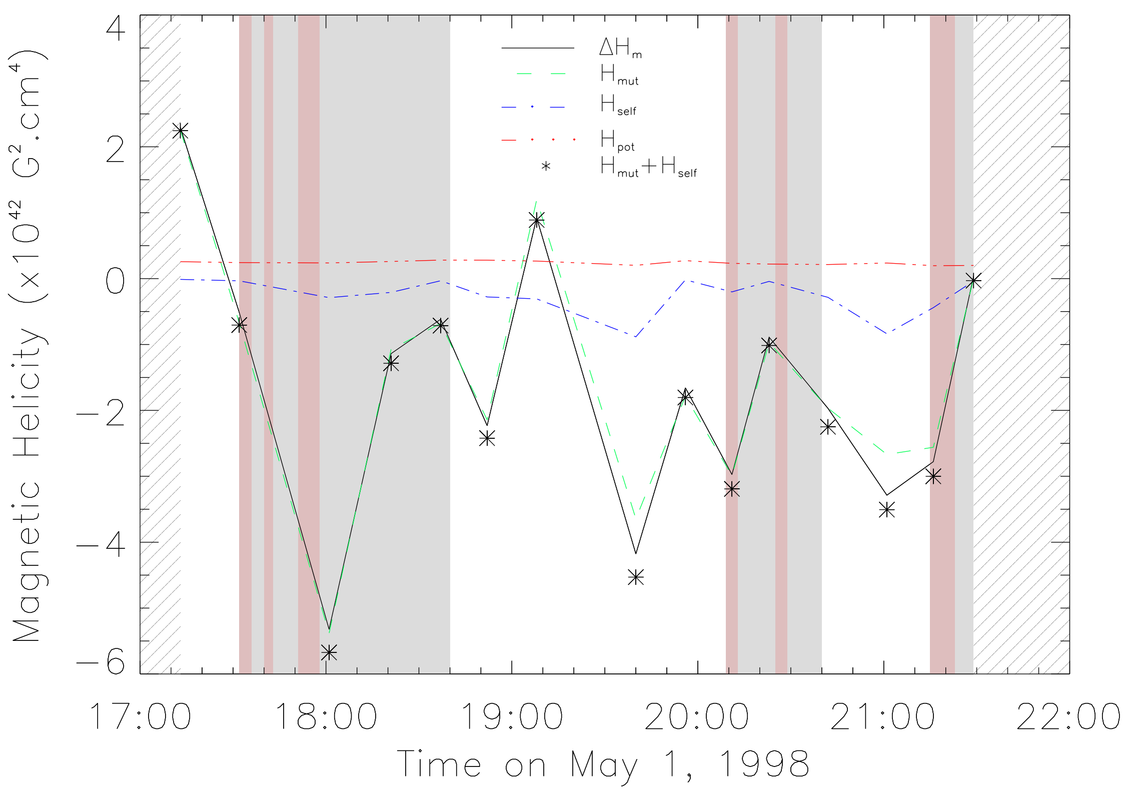

Conclusions (1)

- The self helicity characterises the twist and the writhe of confined flux bundles

- The mutual helicity characterises the crossing of field lines, which also includes large scale twist

- The vacuum helicity can be proxy for the topology of the magnetic configuration (warning: this quantity is not gauge invariant)

Conclusions (2)

What do we need?

- Long time series of vector magnetograms of good quality: good polarization resolution (reduce the noise on the transverse field), higher spatial resolution (to better resolve the polarity inversion line), higher temporal cadence (?): Solar-B, SDO, SOLIS, GREGOR, THEMIS, ATST, ...

- Improving the nonlinear force-free modeling codes. We are working on it!! NLFFF group will meet next month in Stanford

- Need to improve the the correlation photosphere-corona-interplanetary medium: STEREO?